

Identifying young gamma-ray burst fossils

Enrico Ramirez-Ruiz^{★†}

School of Natural Sciences, Institute for Advanced Study, Einstein Drive, Princeton, NJ 08540, USA

Accepted 2004 February 25. Received 2004 February 5; in original form 2003 December 15

ABSTRACT

The recent reports of temporal and spectral peculiarities in the early stages of some afterglows suggest that we may be wrong in postulating a central engine that becomes dormant after the burst itself. A continually decreasing post-burst relativistic outflow, such as put out by a decaying magnetar, may continue to be emitted for periods of days or longer, and we argue that it can be efficiently reprocessed by the ambient soft photon field radiation. Photons produced either by the post-explosion expansion of the progenitor stellar envelope or by a binary companion provide ample targets for the relativistic outflow to interact and produce high-energy γ -rays. The resultant signal may yield luminosities high enough to be detected with the recently launched *INTEGRAL* and the *GLAST* experiment now under construction. Its detection will surely offer important clues for identifying the nature of the progenitor and possibly constraining whether some route other than single-star evolution is involved in producing a rapidly rotating helium core which in turn, at collapse, triggers a burst.

Key words: hydrodynamics – radiation mechanisms: non-thermal – stars: neutron – gamma-rays: bursts.

1 INTRODUCTION

The typical γ -ray burst (GRB) model assumes that the energy input episode is brief, typically $t_{\text{grb}} \leq 1-10^2$ s [see Mészáros (2002) for a recent review]. However, peculiarities in the early stages of some afterglows, e.g. GRB 021004, have served as motivation for considering a more extended input period in which the energy injection continues well beyond t_{grb} (Fox et al. 2003). The enduring activity could in principle emanate from the sluggish drain of orbiting matter into a newly formed black hole (e.g. MacFadyen & Woosley 1999) or from a spin-down millisecond super-pulsar (e.g. Usov 1992), which could produce a luminosity that is, still one day after the burst, as high as $L \sim 10^{47}$ erg s⁻¹. Collapsar (Woosley 1993; Paczyński 1998; MacFadyen & Woosley 1999; Aloy et al. 2000) or magnetar-like GRB models (Usov 1992; Thompson 1994; Wheeler et al. 2000) provide a natural scenario for a sudden burst succeeded by a more slowly decaying energy release (Rees & Mészáros 2000; Ramirez-Ruiz, Celotti & Rees 2002).

The power output would be primarily in a magnetically driven relativistic wind, which would be hugely super-Eddington during the time-scales discussed here. Its luminosity may not dominate the afterglow continuum (Dai & Lu 1998; Zhang & Mészáros 2001), but we argue that it could be efficiently reprocessed into γ -rays. This could be due to the interaction of the post-burst relativistic outflow with the dense soft photon bath arising either from a stellar

companion or from the post-explosion expansion of the remnant shell or supernova (Hjorth et al. 2003; Stanek et al. 2003). The detection of such scattered hard γ -ray radiation would offer the possibility of diagnosing the nature of the precursor star and the compact object that triggers the burst.

2 BINARY SYSTEM WITH A DECAYING MAGNETAR

In the generic pulsar model the field is assumed to maintain a steady value, and the luminosity declines as the spin slows down. However, during the early stages, the magnetic field strength might decline more rapidly than the slowing down time-scale. The power output in this case declines in proportion to B^2 . The spin-down law is given by $-I\Omega\dot{\Omega} = B^2 R^6 \Omega^4 / (6c^3) + 32GI^2 \varepsilon^2 \Omega^6 / (5c^5)$ (Shapiro & Teukolsky 1983), where Ω is the angular frequency, B is the dipolar field strength at the poles, R is the radius of the light cylinder, I is the moment of inertia and ε is the ellipticity of the neutron star. The above decay solution includes both electromagnetic (EM) and gravitational wave (GW) losses. At various times the spin-down will be dominated by one of the loss terms, and one can get approximate solutions. When EM dipolar radiation losses dominate the spin-down, we have $\Omega = \Omega_0(1 + t/t_m)^{-1/2}$. Here

$$t_m = \frac{3c^3 I}{B^2 R^6 \Omega_0^2} \simeq 10^3 I_{45} B_{15}^{-2} P_{0,-3}^2 R_6^{-6} \text{ s} \quad (1)$$

is the characteristic time-scale for dipolar spin-down (e.g. Dai & Lu 1998), $B_{15} = B/(10^{15} \text{ G})$ and $P_{0,-3}$ is the initial rotation period in milliseconds. Here $R_6 = R/10^6$ cm and $I_{45} = I/10^{45}$ g cm².

[★]Chandra Fellow.

[†]E-mail: enrico@ias.edu

When GW radiation losses dominate the spin-down, the evolution is $\Omega \approx \Omega_0(1 + t/t_{\text{gw}})^{-1/4}$, where $t_{\text{gw}} \simeq 1 I_{45}^{-1} P_{0,-3}^4 (\varepsilon/0.1)^{-2}$ s. GW spin-down is important only when the neutron star is born with an initial $\Omega_0 \geq \Omega_* \sim 10^4 \text{ s}^{-1}$ (e.g. Blackman & Yi 1998). When $\Omega_0 < \Omega_*$, the continuous injection luminosity is given by

$$L_m(t) = L_{m,0}(1 + t/t_m)^{-2}, \quad (2)$$

where

$$L_{m,0} = \frac{I\Omega_0^2}{2t_m} \simeq 10^{49} B_{15}^2 P_{0,-3}^{-4} R_6^6 \text{ erg s}^{-1}. \quad (3)$$

If the neutron star is born with $\Omega_0 > \Omega_*$, the time-scale for the GW-dominated regime is short so that Ω will be damped to below Ω_* promptly in a time $t_* = [(\Omega_0/\Omega_*)^4 - 1]t_{\text{gw}}$. After $\Omega < \Omega_*$, GW losses decrease sharply, and the spin-down becomes dominated by the EM losses. The injection luminosity can therefore be divided into two phases, i.e. $L = L_{m,0}/(1 + t/t_{\text{gw}})$ for $t < t_*$ or $L = L_{m,*}/[1 + (t - t_*)/t_{m,*}]^2$ otherwise, where $L_{m,*} = I\Omega_*^2/(2t_m)$ and $t_{m,*} = 3c^3 I/(B^2 R^6 \Omega_*)$.

The bulk of the magnetar energy L_m would be primarily in the form of a magnetically driven, highly relativistic wind consisting of e^- , e^+ and probably heavy ions with $L_\Omega \simeq \zeta L_m$ and $\zeta \leq 1$. We envisage that the burst is triggered by the collapse of a massive star, the helium core of which is presumed to be kept rapidly rotating by spin-orbit tidal interactions with its binary companion. The relativistic (post-burst) wind would then escape the compact remnant while interacting with the soft photon field of the companion with typical energy $\theta = kT/(m_e c^2) \sim 10^{-6} - 10^{-5}$ (i.e. optical and UV frequencies). The scattered photons whose energy is boosted by the square of the bulk Lorentz factor of the magnetized wind (i.e. $\Theta = 2\gamma^2\theta$) propagate in a narrow γ^{-1} beam owing to relativistic aberration. In the case of a mono-energetic isotropic magnetar wind (which is likely to be undisturbed even in the presence of a strong mass outflow from the binary companion: i.e. $L_\Omega/c \gg v\dot{M}$), and assuming that the relativistic particles and soft photons are emitted radially from their source, the energy extracted from a relativistic particle by the inverse Compton process in the Thomson regime is given by $d\gamma(r, \varphi) \simeq -L_* \sigma_T \gamma^2 (1 - \cos \omega)^2 dr / (4\pi m_e \delta^2 c^3)$, where L_* is the luminosity of the stellar companion, ω is the angle between the photon and particle directions before scattering, and r denotes the distance to the magnetar from the volume region where the γ -ray radiation is generated. Here $\delta = \sqrt{\Lambda^2 \sin^2 \varphi + (r - \Lambda \cos \varphi)^2}$ defines the distance from this volume to the companion, Λ is the binary separation, φ is the angle between the lines connecting the binary members and the observer, and $\delta \cos \omega = r - \Lambda \cos \varphi$. The decrease of the Lorentz factor of the particle from the magnetar to infinity is

$$\frac{\Delta\gamma}{\gamma} \simeq 1 - (1 + \zeta\Psi)^{-1}, \quad (4)$$

where

$$\zeta = \frac{\gamma\sigma_T L_*}{4\pi\Lambda m_e c^3} \sim 30 \left(\frac{\gamma}{10^6}\right) \left(\frac{L_*}{10^3 L_\odot}\right) \left(\frac{\Lambda}{R_\odot}\right)^{-1} \quad (5)$$

denotes the efficiency in extracting energy from the relativistic outflow (mainly composed of e^\pm), and $\Psi(\varphi) = [3(\pi - \varphi) - \frac{1}{2} \sin 2\varphi - 4 \sin \varphi]/(2 \sin \varphi)$ is the beaming function of the generated γ -ray radiation.¹ The total luminosity emitted by the relativistic outflowing

¹ Owing to the fact that the optical star is not a point source, $\Psi(\varphi)$ is clearly only accurate for $R_*/\delta < \varphi < \pi - R_*/\delta$, where R_* is the radius of the stellar companion.

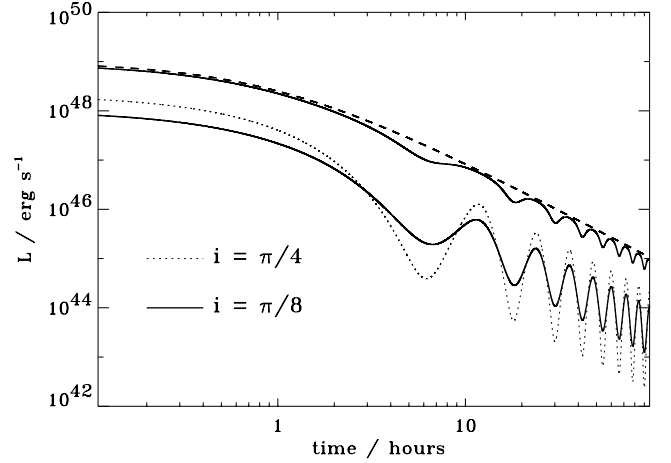


Figure 1. The luminosity emitted by the (post-burst) relativistic outflowing wind through the Compton-drag process. The power output of the magnetically driven relativistic wind declines as the spin slows down (see equation 2) and B is assumed to maintain a steady value (dashed line). $L_{m,0} \simeq 10^{49} \text{ erg s}^{-1}$, $t_m \simeq 10^3 \text{ s}$ and $\zeta = 1$. The luminosity of the γ -ray emission generated as the relativistic outflow interacts with the soft photon field of the companion is shown for $\zeta = 1, 10$ and for two different values of the inclination angle (i.e. i). The period of the binary in the circular orbit is $\tau_p = 12 \text{ h}$. The emitted luminosity was derived under the assumption that the relativistic wind is both steady and mono-energetic. In reality, the properties of the continuing power output could be more complicated. Such effects will certainly enrich the temporal and spectral dependence of the resultant γ -ray emission.

wind through the Compton-drag process in the direction of the observer is highly anisotropic: $L_\Gamma(\varphi) = [\Delta\gamma(\varphi)/\gamma] L_\Omega$. L_Γ strongly varies with φ which in turn changes periodically during orbital motion (i.e. $\cos \varphi = \sin i \cos \nu$ for a circular orbit, where i is the inclination angle and ν is the true anomaly). Fig. 1 shows the luminosity carried by the scattered photons for various positions of the companion and different assumptions regarding the magnetar luminosity.

The Compton drag process can be very efficient in extracting energy from the outflowing relativistic wind provided that $\zeta \geq 1$ (see equation 5). ζ is of course uncertain, but this number does not seem unreasonably high for a progenitor star with a massive binary companion, and suggests that our fiducial value of L_Ω for the overall luminosity need not be an overestimate (Fig. 2). PSR B1259 – 63 is an example of a system where the mildly relativistic outflow from the aged pulsar is thought to interact with the soft photon field radiation produced by its high-mass binary companion (Chernyakova & Illarionov 1999). Since ζ could be less than 10^{-3} for a stellar companion with modest luminosity (or a binary with $\Lambda \gg R_*$), this suggests that we cannot rule out the possibility that part of the γ -ray continuum could still come from the intrinsic pulsed emission from the magnetar itself. For a typical aged pulsar this mechanism yields $L_\Gamma/L_\Omega \sim 10^{-2} - 10^{-3}$ (Arons 1996). The time dependence and spectral properties, in this latter case, will be very distinctive and such effects should certainly be looked for.

2.1 Spectral attributes

If the scenario proposed here is indeed relevant to an understanding of the nature of GRB progenitors, then its existence becomes inextricably linked to both the evolutionary history of the companion and the characteristics of the hydromagnetic wind. The post-burst

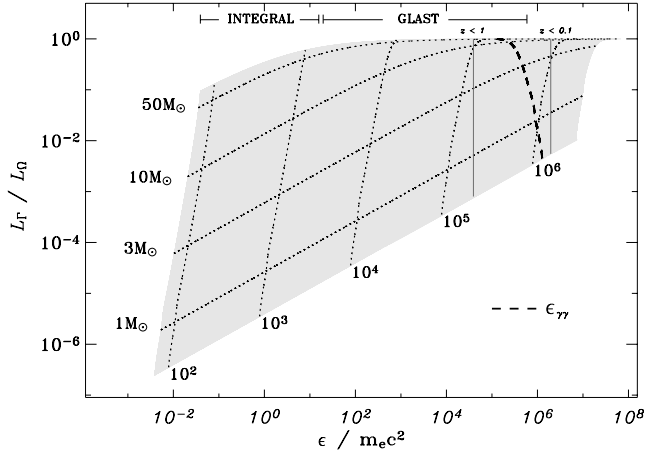


Figure 2. Efficiency in extracting energy from the relativistic outflow as a function of the energy of the scattered γ -ray radiation. The properties of the observed signal are linked to both the evolutionary history of the companion and the bulk Lorentz factor of the relativistic wind (i.e. γ). The main-sequence radii and luminosities of the companion star are calculated using the analytic function derived by Tout et al. (1996). We assume $\Lambda = 3R_*$. The dashed line denotes the threshold energy at which the beamed photons are absorbed by the soft field radiation. The vertical lines denoting where $z < 1$ and $z < 0.1$ are solid lines mark the lower limits to the maximum redshift to which TeV γ -ray sources are visible, based on limits to the background density of infrared/ultraviolet photons (Biller et al. 1998). This has been done for the γ -ray energy range of 0.4–10 TeV, assuming that a source remains *visible* out to an optical depth of 2 and that the majority of the infrared was produced prior to the epoch of the sources under study.

outflow from the compact remnant (which we assume to be highly relativistic) propagates in the soft photon field of the stellar companion where $U(r, \varpi) = m_e c^2 \varpi n_\varpi(r, \varpi)$ is the photon energy density at the location r . As the stellar companion emits a blackbody spectrum, of effective temperature θ_* , the local photon energy density is given by

$$n(r, \varpi) = \frac{2\pi}{hc^3} \left(\frac{m_e c^2}{h} \right)^2 \left[\frac{R_*}{\delta(r)} \right]^2 \frac{\varpi^2}{\exp(\varpi/\theta_*) - 1}, \quad (6)$$

where ϖ is the soft photon energy in units of $m_e c^2$. The scattered photons are boosted by the square of the Lorentz factor so that the local spectrum has a blackbody shape enhanced by γ^2 .

The luminosity of the scattered emission moving along a radial trajectory at an angle φ is $L_r(\gamma, \varphi, \epsilon) = \int_0^\infty \epsilon n_\gamma n_\varpi (1 - \beta \cos \omega) \sigma_{\text{KN}} dV$, where ϵ is the energy of the scattered photons in units of $m_e c^2$, and σ_{KN} is the Klein–Nishina cross-section (Jauch & Rohrlich 1976). As can be seen in Fig. 3, the resulting spectrum is the convolution of all the locally emitted spectra [i.e. $\int_0^\infty dn_\varpi(r, \varpi)$] and it is not one of a blackbody. Note that Klein–Nishina effects are important for incoming photon energies such that $\varpi \gamma (1 + \cos \varphi) > 1$. The maximum energy of the scattered photons in this regime is $\gamma m_e c^2$.

A further effect which may strongly affect the observed spectrum is the production of e^\pm pairs through photon–photon collisions. e^\pm pairs can be produced by scattered photons interacting with the isotropic companion emission or with each other. Photon collisions within the beam itself occur between photons of equal age and can only affect the high-energy tail of the spectrum provided that $\gamma \theta_* > 1/3$ (Svensson 1987). Let us thus consider in turn the role of scattered and companion radiation as seed photons for this process. The interaction between the γ -rays produced

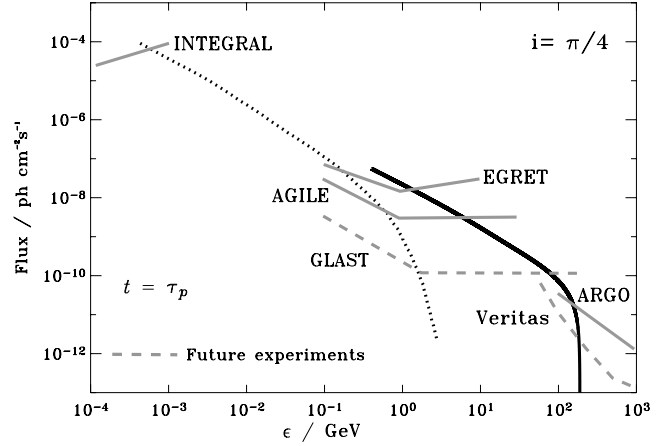


Figure 3. Representative spectra produced by the interaction of the relativistic outflowing wind with the radiation of the stellar companion. The power output of the magnetically driven relativistic wind declines as $(1 + t/t_m)^{-2}$, with $L_{m,0} \simeq 10^{49} \text{ erg s}^{-1}$, $t_m \simeq 10^3 \text{ s}$, $\zeta = 1$ and $t = \tau_p = 12 \text{ h}$ (circular orbit). We assume $z = 0.5$ ($H_0 = 65 \text{ km s}^{-1} \text{ Mpc}^{-1}$, $\Omega_m = 0.3$ and $\Omega_\Lambda = 0.7$). The luminosity of the γ -ray emission is shown for $\gamma = 10^4$ (dotted line), 10^6 (solid line), $\theta_* = 2.5 \times 10^{-6}$ and $\zeta = 1$. The thick grey lines are the predicted sensitivity of a number of operational and proposed instruments in γ -ray astrophysics (Morselli 2002).

by the Compton-drag process and photons emitted by the companion star would occur at large angles, resulting in an average energy threshold of $\epsilon_{\gamma\gamma} > 1/\gamma$. The radiation flux produced at the location r_τ will then decrease by a factor of $\exp[-\tau_{\gamma\gamma}(r_\tau, \epsilon)]$, where $\tau_{\gamma\gamma}(r_\tau, \epsilon) = \int_{\epsilon_{\gamma\gamma}}^\infty d\varpi \int_{r_\tau}^\infty \sigma_{\gamma\gamma}(\varpi, \epsilon) n_\varpi(r, \varpi) dr$ is the photon–photon optical depth and $\sigma_{\gamma\gamma}(\varpi, \epsilon)$ is the corresponding cross-section. As $\sigma_{\gamma\gamma}(\varpi, \epsilon)$ is peaked at the threshold energy (Svensson 1987), the above expression can be simplified to $\tau_{\gamma\gamma}(r_\tau, \epsilon) = (\sigma_T/5) \int_{r_\tau}^\infty \epsilon_{\gamma\gamma} n_\varpi(r, \epsilon_{\gamma\gamma}) dr$, where $n_\varpi(r, \epsilon_{\gamma\gamma})$ is the photon density at threshold at the location r (see equation 6).

As $\varpi \ll \gamma$, this absorption mechanism would be important as long as the companion star produces a sufficient number of photons with energies $\epsilon_{\gamma\gamma} > 1/\gamma$. This limit is illustrated in Fig. 2 for various evolutionary histories of the stellar companion, which has been assumed to be in the main sequence (Izzard, Ramirez-Ruiz & Tout 2004). It can be seen that the number of soft photons able to interact with the high-energy γ -rays to produce e^\pm pairs strongly increases as the bulk Lorentz factor of the relativistic wind exceeds 10^5 . The absorbed radiation will subsequently be reprocessed by the pairs and redistributed in energy. Each electron and positron will have an energy $\gamma_\pm \sim \epsilon/2$ at birth, and will cool as a consequence of the Compton-drag process. The positrons will in turn annihilate in collisions with electrons in the wind, producing a blueshifted annihilation line at $\epsilon \sim \gamma$.

Direct measurements of the characteristics of this hard-energy radiation are frustrated by the fact that, in traversing intergalactic distances, γ -rays may be absorbed by photon–photon pair production on the background field radiation (Gould & Schröder 1967). Photons of energy near 1 TeV interacting with background photons of $\sim 0.5 \text{ eV}$ have the highest cross-section, although a broad range of optical–infrared wavelengths can be important absorbers because the cross-section for pair production is rather broad in energy and, in addition, spectral features in the extragalactic background density can make certain wavebands more important than the cross-section alone would indicate (Biller et al. 1998). The current generation of ground-based, γ -ray telescopes have a typical lower energy

threshold of ~ 0.5 TeV and are thus expected to be able to see sources possessing redshifts up to $z = 0.1$. The next generation of instruments (e.g. *GLAST*²) is expected to have an energy threshold in the region 0.05–0.1 TeV, and will therefore be able to see out to a redshift of at least $z = 0.5$. Fig. 2 and its caption summarize the above limits along with the spectral attributes of the observed γ -ray signal.

3 A DECAYING MAGNETAR IN AN ASYMMETRIC SUPERNOVA REMNANT

The success of the previous model is inseparably linked with the assumed residence of a companion star. Here we consider a related and less restrictive scenario in which the ambient photons are produced by the post-explosion expansion of the disrupted envelope. Photons emitted from the supernova remnant (SNR) shell provide copious targets for the relativistic outflow to interact and produce high-energy γ -rays.

GRBs are thought to be produced when the evolved core of a massive star collapses either to a fast-spinning neutron star or to a newly formed black hole. In the latter case, a GRB is likely to be triggered if the remaining star has sufficient angular momentum to form a centrifugally supported disc (e.g. MacFadyen & Woosley 1999). A funnel along the rotation axis would have been blasted open during the 1–100 s duration of the original burst; it would subsequently enlarge owing to the post-explosion expansion of the envelope of the progenitor star (e.g. Woosley 1993). The ram pressure of the continuing magnetohydrodynamic outflow would further enlarge the funnel. Besides asymmetrically ejecting the SNR envelope (e.g. no ejecta in the polar direction), the supernova explosion may leave behind parts of the He core which take longer in falling back. Additional target photons may arise from parts of the disrupted He core, no longer in hydrostatic equilibrium and moving outwards inside the SNR shell. For a nominal subrelativistic shell speed $v = 10^9 v_9$ cm s⁻¹, the typical distance reached is $r_{\text{snr}} \approx 10^{14} v_9 t_d$ cm in t_d d. The outflowing wind from the compact remnant (which we assume to be relativistic) would propagate inside the funnel cavity (of conical shape with semi-aperture angle ψ) while interacting with the SNR target photons with typical energy $\theta_{\text{snr}} \approx 10^{-6}$ – 10^{-5} (i.e. optical frequencies).

Under the foregoing conditions the particles in the post-burst relativistic outflow see blueshifted photons pouring in from the forward direction. The rate of energy loss of a relativistic particle moving in a radiation with an energy density $w_{\text{snr}} \approx L_{\text{snr}}/2\pi\psi^2 r_{\text{snr}}^2 c$ is about $m_e c^2 d\gamma/dt \approx -w_{\text{snr}} \sigma_T c \gamma^2$ in the Thomson limit. The total luminosity of scattered hard photons L_Γ is equal to the total particle energy losses in the course of motion from the magnetar to infinity: $L_\Gamma(\theta_{\text{snr}}) = [\Delta\gamma(\theta_{\text{snr}})/\gamma]L_\Omega$. L_Γ varies with θ_{snr} which in turn evolves with the expansion history of the stellar envelope. Fig. 4 shows the total luminosity of scattered hard photons L_Γ as a function of the age of the remnant. The bolometric luminosity of SN 1998bw, as derived by Woosley, Eastman & Schmidt (1999), is used here to calculate the photon field energy by assuming a constant expansion velocity of $v = 10^9$ cm s⁻¹. The resulting radiation pressure on electrons in the ejecta will brake any outflow with initial Lorentz factor exceeding some critical value $\gamma_{\text{cd}} \leq (L_\Omega/L_{\text{snr}})^{1/2}$, converting the excess kinetic energy into a directed beam of scattered photons. In reality, the external parts of the post-burst relativistic outflow, which are in closer contact with the funnel walls, are dragged more efficiently since the soft photons arising from the walls can pene-

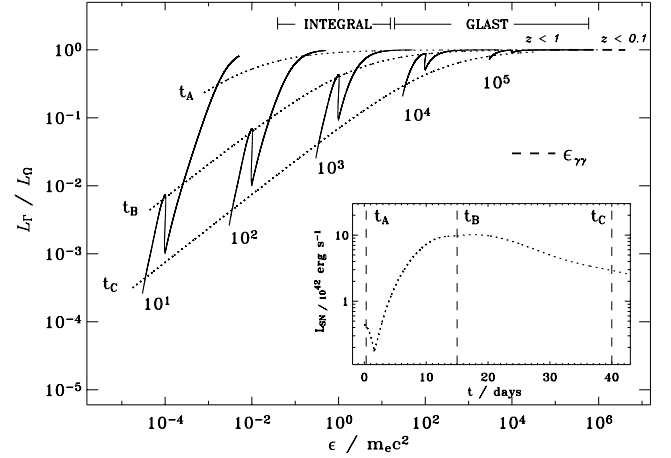


Figure 4. Luminosity of the scattered γ -ray radiation produced by the interaction of the post-burst relativistic outflow with the supernova photon field. The properties of the observed signal are linked to the post-explosion expansion history of the supernova envelope. The bolometric luminosity of SN 1998bw, as derived by Woosley et al. (1999), is used to calculate the photon field energy and column density (inset panel). We assume $v = 10^9$ cm s⁻¹ and $\psi = 0.7$. The thick dashed line denotes the threshold energy at which the beamed photons are absorbed by the radiation from the SNR.

trate only a small fraction of the funnel before being upscattered by relativistic electrons. The outflow itself is then likely to develop a velocity profile with higher Lorentz factor along the symmetry axis, gradually decreasing as the polar angle increases. Moreover, the outflow power may fluctuate; so also may its baryon content, because of entrainment, or because of unsteadiness in the acceleration process at the base of the outflow. In this case, additional γ -rays can be produced in relativistic shocks that develop when fast material overtakes slower material (i.e. internal shocks).

4 DISCUSSION

The initial, energetic portion of the relativistic jet, with a typical burst duration of 10 s, will rapidly expand beyond the envelope of the progenitor star, leading in the usual fashion to shocks and a decelerating blast wave. A continually decreasing fraction of energy may continue being emitted for periods of days or longer, and its reprocessing by the soft photon field radiation can yield a continuum luminosity extending into the γ -ray band. Photons from a binary companion and/or photons entrapped from a supernova explosion provide ample targets for the wind to interact and produce high-energy γ -rays. With a sensitivity of 5×10^{-5} photon cm⁻² s⁻¹ (6×10^{-9} photon cm⁻² s⁻¹) in a $\sim 10^5$ -s exposure, the γ -ray instrument on board *INTEGRAL*³ (*GLAST*) will detect a 10^{47} erg s⁻¹ signal out to a distance of $z \sim 0.5$ (~ 1). A magnetar with $P_0 = 0.8$ ms and $B \sim 10^{14}$ G would lead to $L_\Omega \sim 10^{47}$ erg s⁻¹ after 1 d. This could also be a consequence of a drop in B from 10^{15} to 3×10^{12} G in a compact structure with stored energy of at least 10^{52} erg the characteristic spin period of which remained constant (at a fraction of a millisecond). A similar argument can be developed based on the concept of α -viscosity. For a hot dense torus around a black hole resulting from collapse of the core of the progenitor star, the viscous accretion time for a torus of radius $10^9 r_9$ cm is $t_{\text{vis}} \sim 1.5 r_9^{3/2} B_{12.5}^{-2}$ for $nT \sim \text{constant}$, and the accretion of $\leq 10^{-2} M_\odot$ in $t \sim 1$ d is sufficient to provide a

² <http://www-glast.slac.stanford.edu/>

³ <http://sci.esa.int/home/integral/>

characteristic $L \sim 10^{47}$ erg s $^{-1}$. This luminosity may not dominate the continuum GeV afterglow if it is only modestly reprocessed (i.e. $L_{\Gamma} \leq 10^{44}$ erg s $^{-1}$). In this case, we cannot rule out the possibility that much of the GeV emission is due to inverse Compton (Mészáros & Rees 1994) or synchrotron self-Compton (Derishev, Kocharovsky & Kocharovsky 2001) losses in the standard decelerating blast wave, which could produce an afterglow luminosity that is still, 1 d after the original explosion, as high as 10^{45} erg s $^{-1}$ [see e.g. Dermer, Chiang & Mitman (2000) for a blast wave expanding into a medium with $n_0 = 100$ cm $^{-3}$].

In closing, the scattered γ -rays from a peculiar Ib/c SNR of greater than usual brightness or a high-luminosity stellar companion (i.e. $>10 M_{\odot}$) should be easily detectable (at $t_{\text{obs}} \leq 1.5$ d) by the recently launched *INTEGRAL*. For a less luminous accompanying star (i.e. $<5 M_{\odot}$), the expected γ -ray flux can be detected up to $z = 0.1$, although it may be difficult to disentangle from the scattered SNR emission the intensity of which is likely to dominate at $t \leq 100$ d. The γ -ray signals for ‘mean’ events (i.e. $z \sim 1$) would stand out with high statistical significance above the background provided that $t_{\text{obs}} < 0.1$ – 0.5 d. The planned *GLAST* experiment may also soon provide relevant limits (i.e. $z \leq 0.5$) for individual events at higher threshold energies (Figs 2 and 3). Their detection would unveil the presence of a post-burst relativistic wind, and the spectral signatures of the γ -ray emission would help to constrain the nature of the precursor star.

ACKNOWLEDGMENTS

I gratefully acknowledge very helpful discussions with Martin J. Rees and Aldo Serenelli. I also thank the referee for valuable comments. This research has been supported by NASA through a *Chandra* Postdoctoral Fellowship award PF3-40028.

REFERENCES

- Aloy M. A., Ibanez J. M., Marti J. M., Muller E., MacFadyen A. I., 2000, *ApJ*, 531, L119
 Arons J., 1996, *A&AS*, 120, 49
 Biller S. D. et al., 1998, *Phys. Rev. Lett.*, 80, 2992
 Blackman E. G., Yi I., 1998, *ApJ*, 498, L31
 Chernyakova M. A., Illarionov A. F., 1999, *MNRAS*, 304, 359
 Dai Z. G., Lu T., 1998, *Phys. Rev. Lett.*, 81, 4301
 Derishev E. V., Kocharovsky V. V., Kocharovsky V. I., 2001, *A&A*, 372, 1071
 Dermer C., Chiang J., Mitman K. E., 2000, *ApJ*, 537, 785
 Fox D. W. et al., 2003, *Nat*, 422, 284
 Gould R. J., Schröder G. P., 1967, *Phys. Rev.*, 155, 1408
 Hjorth J. et al., 2003, *Nat*, 423, 847
 Izzard R. G., Ramirez-Ruiz E., Tout C. A., 2004, *MNRAS*, 348, 1215
 Jauch J. M., Rohrlich F., 1976, *The Theory of Protons and Electrons*, 2nd edn. Springer, New York
 MacFadyen A. I., Woosley S. E., 1999, *ApJ*, 524, 262
 Mészáros P., 2002, *ARA&A*, 40, 137
 Mészáros P., Rees M. J., 1994, *MNRAS*, 269, L41
 Morselli A., 2002, *Surveys in High Energy Physics*, 16, 255
 Paczynski B., 1998, *ApJ*, 494, L45
 Ramirez-Ruiz E., Celotti A., Rees M. J., 2002, *MNRAS*, 337, 1349
 Rees M. J., Mészáros P., 2000, *ApJ*, 545, L73
 Shapiro S. L., Teukolsky S. A., 1983, *Black Holes, White Dwarfs, and Neutron Stars: The Physics of Compact Objects*. Wiley, New York
 Stanek K. et al., 2003, *ApJ*, 591, L17
 Svensson R., 1987, *MNRAS*, 227, 403
 Thompson C., 1994, *MNRAS*, 270, 480
 Tout C. A., Pols O. R., Eggleton P. P., Zhanwen H., 1996, *MNRAS*, 281, 252
 Usov V. V., 1992, *Nat*, 357, 472
 Wheeler J. G., Yi I., Hoflich P., Wang L., 2000, *ApJ*, 537, 810
 Woosley S. E., 1993, *ApJ*, 405, 273
 Woosley S. E., Eastman R. G., Schmidt B., 1999, *ApJ*, 516, 788
 Zhang B., Mészáros P., 2001, *ApJ*, 552, L35

This paper has been typeset from a $\text{\TeX}/\text{\LaTeX}$ file prepared by the author.